LAWRENCE
LIVERMORE
NATIONAL
LABORATORY

UCRL-CONF-235082

Progress Towards Optimally Efficient Schemes for Monte Carlo Thermal Radiation Transport

R. P. Smedley-Stevenson, E. D. Brooks III

September 28, 2007

Winter 2007 meeting of the American Physical Society
Washington, DC, United States
November 11, 2007 through November 15, 2007

Progress Towards Optimally Efficient Schemes for Monte Carlo Thermal Radiation Transport, invited

Richard P. Smedley-Stevenson[1] and Eugene D. Brooks III[2]

[1]*AWE, Aldermaston, Reading, RG7 4PR, UK, richard.smedley-stevenson@awe.co.uk*
[2]*University of California, Lawrence Livermore National Laboratory, P. O. Box 808, Livermore, CA 94550, USA, brooks3@llnl.gov*

INTRODUCTION

In this summary we review the complementary research being undertaken at AWE and LLNL aimed at developing optimally efficient algorithms for Monte Carlo thermal radiation transport based on the difference formulation. We conclude by presenting preliminary results on the application of Newton-Krylov methods for solving the Symbolic Implicit Monte Carlo (SIMC) energy equation.

THE DIFFERENCE FORMULATION

In the difference formulation instead of solving for the radiation intensity I in the Monte Carlo simulation, we instead model the departure of the intensity from its equilibrium value $D = I - B$, where B is the blackbody radiation energy density [1]. The difference intensity D tends to zero in the equilibrium diffusion limit, hence this transformation significantly reduces the variance of the Monte Carlo solution in optically thick regions without altering the transport problem. More generally we can formulate the transport problem in terms of an arbitrary offset function B_{DF}.

For a pure absorber in slab geometry with an opacity which does not depend on frequency, the coupled system of equations in the generalized difference formulation can be written as:

$$\left(\frac{1}{c}\frac{\partial}{\partial t} + \underline{\Omega}\cdot\nabla + \sigma_a\right)D = \sigma_a\left(B - B_{DF}\right) - \frac{1}{c}\frac{\partial B_{DF}}{\partial t} - \underline{\Omega}\cdot\nabla B_{DF} \qquad (1)$$

$$\rho C_V \frac{\partial T}{\partial t} = \int_{4\pi}\sigma_a D\, d\Omega - \sigma_a\left(B - B_{DF}\right)$$

where c is the speed of light, $\underline{\Omega}$ is the propagation direction, σ_a is the absorption opacity and $B = acT^4$, where a is the radiation constant and T is the temperature of the medium. Here we have assumed that the medium is in local thermodynamic equilibrium and also that it has a constant specific heat capacity, ρC_V.

The difference formulation contains two additional source terms, the first related to the time evolution of the offset function and the second corresponding to spatial variation of the offset function. For an isotropic offset function the latter term makes zero net contribution to the energy in the problem, and the Monte Carlo sampling scheme can preserve this property by emitting pairs of particles with equal weights of opposite sign, sampled according to a cosine distribution relative to the direction of the gradient.

Initial studies of the difference formulation have focused on an SIMC treatment of the time evolution behavior. Attempts to couple the difference formulation to the IMC method are reviewed at the end of this section.

Piecewise-Linear Formulations

To simplify the implementation the difference formulation was originally studied in the context of a piecewise constant spatial discretisation [2]. This is well known to produce results with excessive numerical diffusion for problems with optically thick cells, due to the jump terms used to represent the gradient of the blackbody function. Physically correct behavior can be obtained by introducing a piecewise linear finite element representation of either the material temperature or the blackbody energy density [3,4]. Alternatively, it is possible to treat both quantities as having a linear variation, requiring consistency between the two representations only at the nodes of each element [5].

The penalty for introducing a linear variation is the additional complexity inherent in the algorithms and the growth in the number of unknowns for discontinuous representations. Furthermore, it is desirable to maintain a piecewise constant discretisation of the material temperature as this simplifies the coupling of the transport algorithm to hydrodynamics codes in order to solve complex coupled radiation-hydrodynamics problems.

It is possible to re-introduce a linear variation into the blackbody function in the gradient source term, in order to improve the accuracy of the equilibrium radiation flux, while leaving the remaining terms unchanged and still obtain the correct diffusion limit behavior [6]. This is illustrated in figure 1, where we reproduce the results for an initially cold purely absorbing slab (with $\sigma_a = 200\,\text{cm}^{-1}$ and specific heat capacity 10^8 J/cm-keV)

heated by an isotropic source of radiation corresponding to a temperature of 1 keV applied at the left hand end.

Generalized Offset Functions

In addition to examining the behavior in opaque media, an attempt has been made to quantify the efficiency of the difference formulation for problems with optically thin cells by introducing a cost function associated with the integral of the magnitude of the sources in the transport equation [5]. Monte Carlo noise in the blackbody field has been shown to significantly degrade the efficiency of the difference formulation in transparent regions, rendering it more expensive than using a zero offset function; this is due to the difficulties obtaining accurate values for the spatial derivative terms when the solution is contaminated with statistical noise. An optimal difference scheme must be more flexible than simply using the local value of the blackbody function in the offset function.

The use of generalized offset functions has been investigated in the context of producing a scheme with improved computational performance, for problems containing transparent regions and exhibiting significant non-equilibrium behavior [5]. This has led to several profitable avenues for future research. In particular, the introduction of a linearly anisotropic term into the offset function offers the potential for even greater performance gains from the difference formulation in optically thick regions modeled with linear elements.

This additional term accounts for the linearly anisotropic component of the radiation field in the diffusion limit, which was previously being ignored. It eliminates the within-cell gradient term, removing the need to create uniformly distributed particle pairs in the cell interior. The particle sources are concentrated at the cell interfaces, as in the piecewise constant scheme, but now they are accurately modeling the diffusive energy flow by virtue of the spatial gradient of this additional term.

Contributions to the cost function are shown in figure 2 for an initially cold purely absorbing slab (with $\sigma_a = \rho C_V = c = a = 1$), with an isotropic inward source of radiation corresponding to a drive temperature of $\sqrt{2}$ is incident on the left hand end. This figure illustrates the dramatic reduction in computational work associated with the use of the following offset function:

$$B_{DF} = B - h\sigma_a^{-1}\underline{\Omega}\cdot\nabla B \qquad (2)$$

Here h is a piecewise constant function in the range [0,1] which minimizes the local value of the spatial gradient source terms. As the radiation wave penetrates deeper into the slab, the cost function for this scheme (bold curve) asymptotes towards a $t^{-½}$ variation (provided that we use a fully implicit value of the blackbody function in this offset function). We contrast this with the $t^{½}$ behavior of the intensity scheme (the curve labeled SIMC emission source).

Another significant idea is to treat the offset function in the difference formulation explicitly [5]. For the SIMC method this eliminates the additional implicit terms in the energy equation that arise from the difference formulation source terms. These are based on differences between the values of neighboring unknowns and are therefore difficult to estimate a priori. Their presence makes the solution of the SIMC energy equation more difficult, by reducing the diagonal dominance and increasing the bandwidth of the matrix associated with the energy deposition.

A further consequence is that the use of an explicit offset function makes it possible to combine the difference formulation with an IMC temporal discretisation in the manner described by Gentile [7]; each particle now has a known weight at the start of the tracking step, unlike the symbolic weights carried by the particles in the SIMC method, and there is no system of equations to solve for the energy balance. Unfortunately, the variance of the difference intensity increases dramatically due to the extension of the lifetime of the particles affected by the IMC method; the majority of absorptions and re-emission events in opaque cells are modeled as scattering events, with a mean free path derived from the absorption coefficient.

Particles emitted by the gradient term have their direction randomized at the first scattering event and have lost all knowledge of the direction of the background energy flow associated with the equilibrium radiation flux. After the first collision these particles cease to carry any useful information about the difference field, but the fact that there are an almost equal number of positive and negative particles means that they represent a significant source of additional variance for the energy deposition tallies. The resulting computational scheme can be significantly more expensive that the original intensity formulation [5].

SIMC ENERGY EQUATION

Current research is focused on the development of efficient multi-dimensional algorithms on massively parallel computer platforms. To employ the difference formulation in multi-dimensions we have to be able to efficiently solve the non-linear SIMC energy equation in parallel. Initial investigations at AWE have focused on the performance of Newton-Krylov algorithms for solving the

non-linear energy equation associated with a simple 1D test problem. The non-linear equations are solved using the PETSc SNES non-linear solver package [8], with an interface to the ML [9] and BoomerAMG [10] algebraic multi-grid solvers to enable them to be employed as preconditioners.

This test problem is a variant of the previous problem and consists of a purely absorbing slab of length 20 divided into two equal regions with unit cross-section in the left hand region and $\sigma = 10$ in the right hand region. Otherwise the properties of the medium and the radiation drive are identical to those of the previous problem used to test generalized offset functions. By modeling a finite slab and allowing radiation to escape from the right-hand end of the medium, we allow this problem to reach steady-state.

We investigate the solution of the energy equation for the first time-step of an SIMC calculation, employing a large time-step (1000) to ensure that most entries in the energy deposition matrix are populated; this makes the non-linear problem extremely challenging to solve. We compare the performance for meshes with 200 and 400 uniform cells, for both piecewise constant and piecewise linear elements. The results are presented in table 1 for a variety of different preconditioning and update strategies for the Jacobian and/or the preconditioning matrix during the Newton-Krylov iterations, treating either the blackbody energy density or the material temperature as the unknown during the iterations. The former leads to superior performance, as the corresponding Jacobian matrix exhibits significantly less variability; only the diagonal entries vary with temperature and this variation is suppressed for large time-steps.

The ILU(0) preconditioner produces the best performance for this small 1D test problem. The convergence behavior is almost identical to that of the direct solver and this provides a standard by which we can measure the effectiveness of the other preconditioners. The number of Krylov solver iterations for the ML preconditioner is identical to the ILU(0) preconditioner, indicating that it is equally effective at accelerating the Newton-Krylov iterations. This is important, as the scalability of multi-grid preconditioners has already been demonstrated on 10,000s of processors, while parallel implementations of the ILU(0) preconditioner (based on coloring algorithms) permit only modest levels of parallelism. To summarize, results so far look promising in terms of finding a robust and scalable parallel preconditioner for a solution of the SIMC energy equation based on Newton-Krylov methods. This is an important step towards developing an efficient multi-dimensional implementation of the difference formulation based on the SIMC method.

REFERENCES

1. A. SZÖKE AND E. D. BROOKS III, "The Transport Equation in Optically Thick Media", *Journal of Quantitative Spectroscopy and Radiative Transfer*, **91**, 95 (2005).
2. E. D. BROOKS III, M. S. MCKINLEY, F. DAFFIN and A. SZÖKE, "Symbolic Implicit Monte Carlo Radiation Transport in the Difference Formulation: A Piecewise Constant Discretisation," *Journal of Computational Physics*, **205**, 737 (2005).
3. J.-F. CLOUET AND G. SAMBA, "Asymptotic Diffusion Limit of the Symbolic Monte-Carlo Method for the Transport Equation," *Journal of Computational Physics*, **195**, 293 (2004).
4. E.D. BROOKS III, A. SZÖKE, and J.D.L. PETERSON, "Piecewise Linear Discretization of Symbolic Implicit Monte Carlo Radiation Transport in the Difference Formulation," ", *Journal of Computational Physics*, **220**, 471 (2006).
5. R. P. SMEDLEY-STEVENSON, "Improved Implicit Monte Carlo Schemes Based on the Difference Formulation", *Proc. of the M&C+SNA 2007 meeting,* Monterey, CA, USA, April 15–19, published on CD-ROM by the American Nuclear Society, La Grange Park, Illinois, USA (2007).
6. T. LUU, E.D. BROOKS III and A. SZÖKE, "Source Tilting in the Difference Formulation for Radiation Transport", submitted to Journal of Computational Physics.
7. N. A. GENTILE, "The Difference Formulation of Radiation Transport in Implicit Monte Carlo", *Transactions of the American Nuclear Society*, **95**, 871 (2006).
8. S. BALAY, W. D. GROPP, L. C. MCINNES and B. F. SMITH, "PETSC home page", http://www.mcs.anl.gov/petsc, (2001).
9. M. W. GEE, C. M. SIEFERT, J. J. HU, R. S. TUMINARO and M. G. SALA, "ML 5.0 Smoothed Aggregation User's Guide", SAND2006-2649, Sandia National Laboratories (2006).
10. http://www.llnl.gov/CASC/hypre.

This work was performed under the auspices of the U. S. Department of Energy by University of California, Lawrence Livermore National Laboratory under Contract W-7405-Eng-48.

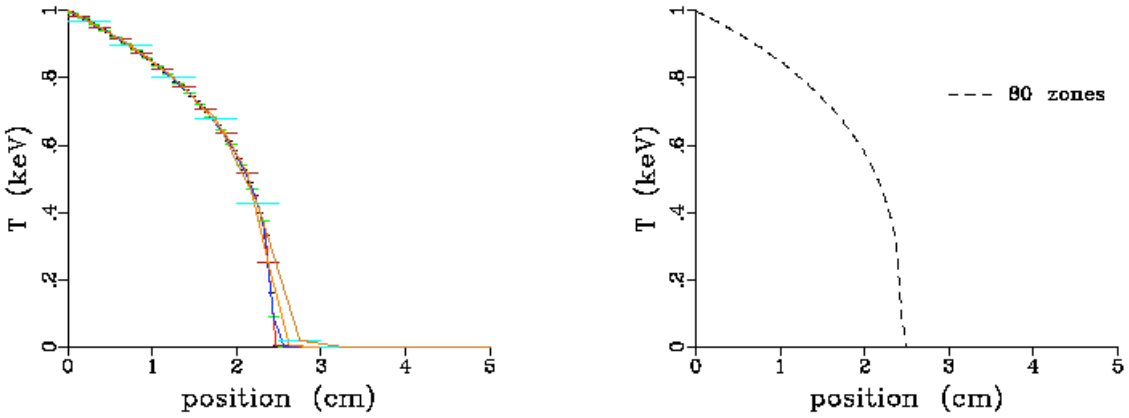

Fig. 1. The left panel shows an overlay of calculations using a source tilt based interpolation between neighboring element centers for 12.5, 25, 50, and 100 mean free paths per zone at $t = 3\times10^{-7}$ s. Lines have been connected between centers of the zones to facilitate comparison with the right-hand panel, which shows an analogous 80 zone (12.5 mean free paths per zone) self-consistent piecewise-linear calculation.

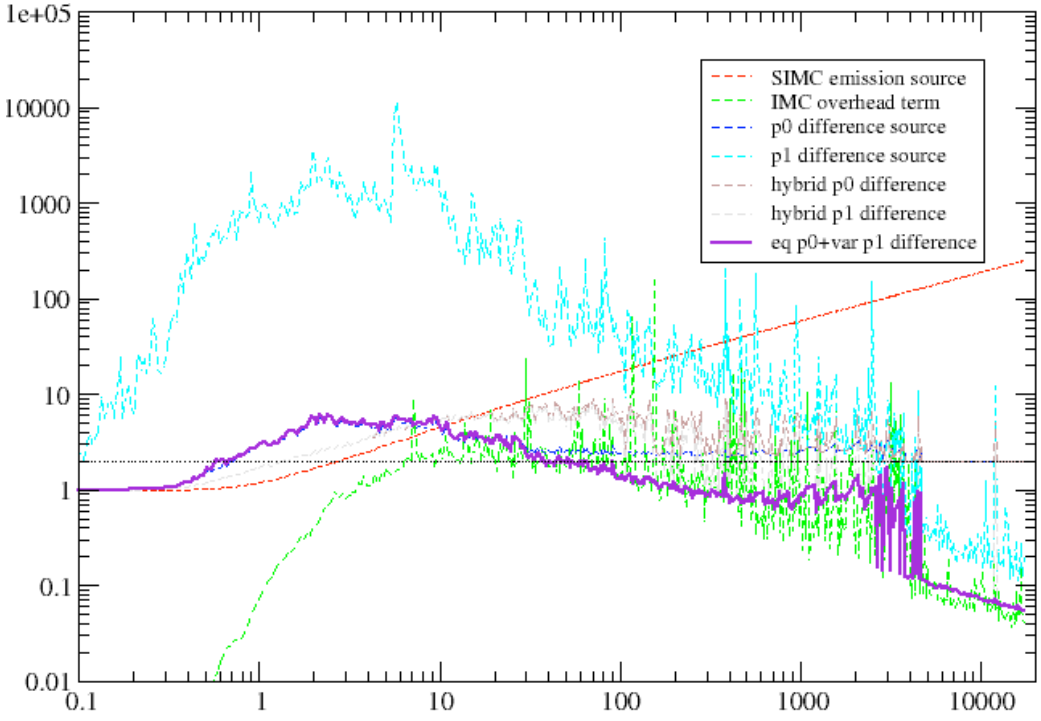

Fig. 2. Contributions to the cost function verses time. The implicitness of the offset function is adapted to minimize the number of particles emitted during the time-step, which accounts for the jumps which occur in the region $t = 2000 - 5000$ due to switching from the explicit to a fully implicit scheme. The cost of the scheme used to generate the statistics is shown as the bold purple curve, while the other curves represent hypothetical contributions to the cost function for different choices of offset function derived from the same particle statistics.

Blackbody energy density as the unknown

Preconditioner for GMRES(30)	200 Piecewise constant elements, Jacobian/Preconditioner update Strategy: No updates									200 Piecewise linear elements, Jacobian/Preconditioner update Strategy: No updates								
	Jac. only						Jac.+Pre.			Jac. only						Jac.+Pre.		
LU	6	12	0.05	4	12	0.06	3	6	0.09	12	24	0.17	5	17	0.21	4	8	0.39
ILU(0)	6	12	0.07	4	12	0.07	3	6	0.06	12	24	0.14	5	17	0.19	4	8	0.29
None	8	823	0.21	6	922	0.26	6	922	0.27	12	1107	0.57	9	1204	0.74	9	1204	0.85
Jacobi	9	726	0.19	7	764	0.23	7	800	0.26	12	960	0.51	6	749	0.49	6	752	0.56
SOR	8	170	0.10	6	135	0.11	6	135	0.13	13	347	0.50	9	232	0.50	9	232	0.59
ML	6	12	0.12	4	12	0.13	3	6	0.21	12	24	0.34	5	17	0.31	4	8	0.58
BoomerAMG	7	26	0.13	4	17	0.15	4	17	0.16	23	70	0.62	6	38	0.49	5	31	0.67

Preconditioner for GMRES(30)	400 Piecewise constant elements, Jacobian/Preconditioner update Strategy: No updates									400 Piecewise linear elements, Jacobian/Preconditioner update Strategy: No updates								
	Jac. only						Jac.+Pre.			Jac. only						Jac.+Pre.		
LU	7	14	0.15	4	11	0.23	3	6	0.32	20	40	0.84	7	18	1.14	6	12	3.19
ILU(0)	7	14	0.16	4	11	0.16	3	6	0.22	20	40	0.72	7	20	0.97	6	12	2.17
None	9	1005	0.56	6	875	0.56	6	875	0.62	17	919	1.43	8	901	1.80	8	901	2.25
Jacobi	10	868	0.47	7	887	0.57	7	804	0.62	18	860	1.34	10	777	1.83	10	706	2.23
SOR	10	312	0.45	7	207	0.43	7	207	0.51	19	320	1.93	7	219	1.75	7	219	3.44
ML	7	14	0.24	4	11	0.36	3	6	0.40	20	40	1.71	7	20	1.63	6	12	3.11
BoomerAM G	7	22	0.30	5	17	0.29	5	17	0.56	*35*	*86*	*3.08*	7	45	1.99	7	44	4.00

Material temperature as the unknown

Preconditioner for GMRES(30)	200 Piecewise constant elements, Jacobian/Preconditioner update Strategy: No updates									200 Piecewise linear elements, Jacobian/Preconditioner update Strategy: No updates								
	Jac. only						Jac.+Pre.			Jac. only						Jac.+Pre.		
LU	584	1168	1.10	12	122	0.16	8	16	0.21	2433	4866	11.6	14	279	0.60	10	20	0.95
ILU(0)	584	1168	1.15	12	122	0.16	8	16	0.16	2433	4866	16.9	14	279	0.70	10	20	0.70
None	*386*	*1672*	*0.83*	14	1121	0.35	14	1121	0.40	*29*	*132*	*0.22*	13	1823	1.10	13	1823	1.26
Jacobi	*968*	*3003*	*1.82*	20	1105	0.38	16	590	0.30	*22*	*60*	*0.19*	16	1919	1.21	14	835	0.87
SOR	*22*	*61*	*0.11*	11	331	0.23	*23*	*66*	*0.28*	*12*	*27*	*0.18*	16	620	1.09	*18*	*62*	*0.70*
ML	584	1168	3.86	12	122	0.50	8	16	0.35	2433	4866	4.51	14	279	2.24	10	20	1.19
BoomerAMG	583	1166	3.06	12	126	0.39	8	19	0.27	2438	4876	4.42	13	292	2.24	9	23	1.00

Preconditioner for GMRES(30)	400 Piecewise constant elements, Jacobian/Preconditioner update Strategy: No updates									400 Piecewise linear elements, Jacobian/Preconditioner update Strategy: No updates								
	Jac. only						Jac.+Pre.			Jac. only						Jac.+Pre.		
LU	924	1848	5.84	14	190	0.54	9	18	0.91	5844	11688	103	15	449	3.26	11	22	5.86
ILU(0)	924	1848	8.12	14	190	0.56	9	18	0.65	5844	11688	121	15	449	3.72	11	22	5.05
None	5219	20545	34.6	13	1290	0.89	13	1290	1.04	*31*	*148*	*0.62*	13	2859	4.59	13	2859	8.00
Jacobi	*95*	*297*	*0.43*	18	1473	1.06	20	667	0.97	*18*	*46*	*0.46*	22	3112	6.86	18	773	3.34
SOR	*105*	*305*	*1.88*	13	677	1.10	*41*	*108*	*1.45*	*10*	*26*	*0.52*	16	1066	6.72	58	4557	37.4
ML	924	1848	17.8	14	190	1.67	9	18	1.08	5844	11688	405	15	449	14.7	11	22	7.42
BoomerAMG	926	1852	14.3	13	179	1.40	9	24	0.94	5860	11721	361	13	430	11.6	10	27	4.88

Table 1. Number of Newton iterations, Krylov solver iterations and CPU time measured in seconds (on a single IBM PWR3 processor) for the solution of the SIMC energy equation, for a simple slab geometry test case. Entries shown in italics correspond to cases where the iteration was terminated prematurely due to a line search failure.